JNS

CLINICAL ARTICLE

J Neurosurg 136:1371–1380, 2022

Use of probabilistic tractography to provide reliable distinction of the motor and sensory thalamus for prospective targeting during asleep deep brain stimulation

Jennifer Muller, MS,[1,2] Mahdi Alizadeh, PhD,[1,2] Caio M. Matias, MD, PhD,[1] Sara Thalheimer, BA,[1] Victor Romo, MD,[3] Justin Martello, MD,[4] Tsao-Wei Liang, MD,[5] Feroze B. Mohamed, PhD,[2] and Chengyuan Wu, MD, MSBmE[1,2]

[1]Department of Neurological Surgery, Vickie and Jack Farber Institute for Neuroscience, Thomas Jefferson University, Philadelphia, Pennsylvania; [2]Jefferson Integrated Magnetic Resonance Imaging Center, Department of Radiology, Thomas Jefferson University, Philadelphia, Pennsylvania; [3]Department of Anesthesia, Thomas Jefferson University, Philadelphia, Pennsylvania; [4]Department of Neurology, Christiana Care Health System, Newark, Delaware; and [5]Department of Neurology, Thomas Jefferson University, Philadelphia, Pennsylvania

OBJECTIVE Accurate electrode placement is key to effective deep brain stimulation (DBS). The ventral intermediate nucleus (VIM) of the thalamus is an established surgical target for the treatment of essential tremor (ET). Retrospective tractography-based analysis of electrode placement has associated successful outcomes with modulation of motor input to VIM, but no study has yet evaluated the feasibility and efficacy of prospective presurgical tractography-based targeting alone. Therefore, the authors sought to demonstrate the safety and efficacy of probabilistic tractography–based VIM targeting in ET patients and to perform a systematic comparison of probabilistic and deterministic tractography.

METHODS Fourteen patients with ET underwent preoperative diffusion imaging. Probabilistic tractography was applied for preoperative targeting, and deterministic tractography was performed as a comparison between methods. Tractography was performed using the motor and sensory areas as initiation seeds, the ipsilateral thalamus as an inclusion mask, and the contralateral dentate nucleus as a termination mask. Tract-density maps consisted of voxels with 10% or less of the maximum intensity and were superimposed onto anatomical images for presurgical planning. Target planning was based on probabilistic tract-density images and indirect target coordinates. Patients underwent robotic image-guided, image-verified implantation of directional DBS systems. Postoperative tremor scores with and without DBS were recorded. The center of gravity and Dice similarity coefficients were calculated and compared between tracking methods.

RESULTS Prospective probabilistic targeting of VIM was successful in all 14 patients. All patients experienced significant tremor reduction. Formal postoperative tremor scores were available for 9 patients, who demonstrated a mean 68.0% tremor reduction. Large differences between tracking methods were observed across patients. Probabilistic tractography–identified VIM fibers were more anterior, lateral, and superior than deterministic tractography–identified fibers, whereas probabilistic tractography–identified ventralis caudalis fibers were more posterior, lateral, and superior than deterministic tractography–identified fibers. Deterministic methods were unable to clearly distinguish between motor and sensory fibers in the majority of patients, but probabilistic methods produced distinct separation.

CONCLUSIONS Probabilistic tractography–based VIM targeting is safe and effective for the treatment of ET. Probabilistic tractography is more precise than deterministic tractography for the delineation of VIM and the ventralis caudalis nucleus of the thalamus. Deterministic algorithms tended to underestimate separation between motor and sensory fibers, which may have been due to its limitations with crossing fibers. Larger studies across multiple centers are necessary to further validate this method.

https://thejns.org/doi/abs/10.3171/2021.5.JNS21552

KEYWORDS deep brain stimulation; essential tremor; prospective targeting; probabilistic tractography; deterministic tractography; functional neurosurgery

ABBREVIATIONS CoG = center of gravity; DBS = deep brain stimulation; DSC = Dice similarity coefficient; DWI = diffusion-weighted imaging; ET = essential tremor; GPU = graphics processing unit; PM = probability map; TDI = tract-density image; TETRAS = The Essential Tremor Rating Assessment Scale; VC = ventralis caudalis nucleus; VIM = ventral intermediate nucleus.

SUBMITTED March 4, 2021. **ACCEPTED** May 11, 2021.
INCLUDE WHEN CITING Published online October 8, 2021; DOI: 10.3171/2021.5.JNS21552.

©AANS 2022, except where prohibited by US copyright law

Brought to you by Thomas Jefferson University | Unauthenticated | Downloaded 10/07/26 03:23 PM UTC

Deep brain stimulation (DBS) of the ventral intermediate nucleus (VIM) of the thalamus is an established surgical treatment of essential tremor (ET) and tremor in patients with Parkinson's disease.[1] Accurate presurgical visualization of VIM remains one of the major challenges for this target.[2] Inaccurate electrode position can result in incomplete clinical benefit, but the optimal target location for maximum clinical benefit has been shown to vary between individuals.[1,3] Because the thalamus lacks sufficient intrinsic contrast on current standard clinical MRI,[4] VIM is not readily visible on the sequences typically used in DBS planning.[5,6] Therefore, surgical targeting has primarily relied on the use of indirect targeting methods, in which the target is determined on the basis of its standard relationship with the midcommissural point.[4] Although it provides a useful estimate,[7,8] indirect targeting is relatively insensitive to individual variations in size, location, and configuration of thalamic nuclei. As such, it has become common practice to require awake physiological mapping to determine final electrode placement.

Reliable techniques that can be used to directly visualize and target the VIM and other thalamic nuclei on a patient-specific basis have been the subject of active research over the past decade.[4] Diffusion-weighted imaging (DWI) is a noninvasive tool for visualizing white matter pathways in the human brain[9] and has been suggested as a way to visualize the various subdivisions of the thalamus that are possible target locations,[9,10] including the VIM for presurgical targeting.[11–14] Moreover, DWI-based methods can also localize adjacent regions associated with stimulation-induced adverse effects as a means to define safety margins and avoid possible adverse effects.[10] The ventralis caudalis nucleus (VC) of the thalamus lies immediately posterior to VIM, and stimulation of VC produces paresthesias in the corresponding part of the body.[15]

Diffusion tractography algorithms can be classified as deterministic and probabilistic. Deterministic tractography is currently the only method available in commercial neurosurgical planning software and simplifies the fiber path across a given voxel as a single dominant direction.[16,42] However, utilization of only one diffusion orientation per voxel may not adequately characterize voxels that contain crossing, branching, or fanning fibers.[17] Studies have estimated that approximately 90% of white matter voxels contain crossing fibers.[18] As a result, deterministic methods may follow false tracts or stop in regions with isotropic tensors.[19] Although more computationally demanding, probabilistic tractography retains multidirectional anisotropic information and is thus able to identify multiple streamlines and their relative probabilities. This method has the advantage of showing greater sensitivity to overlapping fibers.[16] However, probabilistic tractography can be both computationally demanding and difficult to interpret and is therefore currently only available in research software.[4]

On the basis of prior retrospective studies that illustrated the efficacy of modulation of motor input to VIM for tremor control,[5] we have incorporated probabilistic tractography–based targeting into our routine clinical practice. At the same time, a systematic comparison of probabilistic versus deterministic tractography techniques for thalamic parcellation is crucial to increasing the accuracy of tractography-based targeting. In this study, we report the clinical results of using probabilistic tractography to prospectively target the VIM region in a cohort of 14 ET patients who underwent DBS, as well as the results of our systematic comparison of probabilistic and deterministic tractography.

TABLE 1. Patient information and programming parameters for probabilistic tractography–based VIM targeting (n = 14)

Characteristic	Value
Patient information	
Age at surgery, yrs	66.2 ± 7.3
Sex	
Male	8
Female	6
Disease duration, yrs	16.1 ± 16.2
Age at diagnosis, yrs	49.7 ± 18.8
Programming parameters	
Amplitude, mA	1.89 ± 0.91 (0.35–4.00)
Frequency, Hz	160 ± 28 (128–220)
Pulse width, μsec	56 ± 16 (20–90)
Directional programming, %	48.1

Values are shown as mean ± SD, number, or mean ± SD (range).

Methods

Starting in August 2018, we began to incorporate probabilistic tractography–based VIM targeting into preoperative planning for DBS. Probabilistic tractography was selected given the decussation of the dentatorubrothalamic tract and the limitations of deterministic tractography for capturing crossing fibers. Patients underwent robotic image-guided, image-verified implantation of directional DBS systems. Qualitative improvement of tremor or quantitative tremor scores (based on The Essential Tremor Rating Assessment Scale [TETRAS][20]) were recorded with and without DBS during routine clinical practice. TETRAS evaluates the presence and severity/amplitude of tremor in the head, face, tongue, voice, upper limb, and lower limb, as well as during tasks such as drawing spirals, handwriting, dot approximation, and standing. We subsequently performed a retrospective comparative analysis of probabilistic and deterministic tractography–based VIM targeting. This study received ethical approval by the local institutional review board for retrospective review of clinical and imaging data.

Patient Cohort

Fourteen patients with refractory ET who were deemed appropriate candidates for DBS according to standard clinical criteria underwent DBS with probabilistic tractography–based VIM targeting (Table 1).

Image Acquisition

To eliminate potential movement artifacts and to maxi-

Brought to you by Thomas Jefferson University | Unauthenticated | Downloaded 10/07/26 03:23 PM UTC

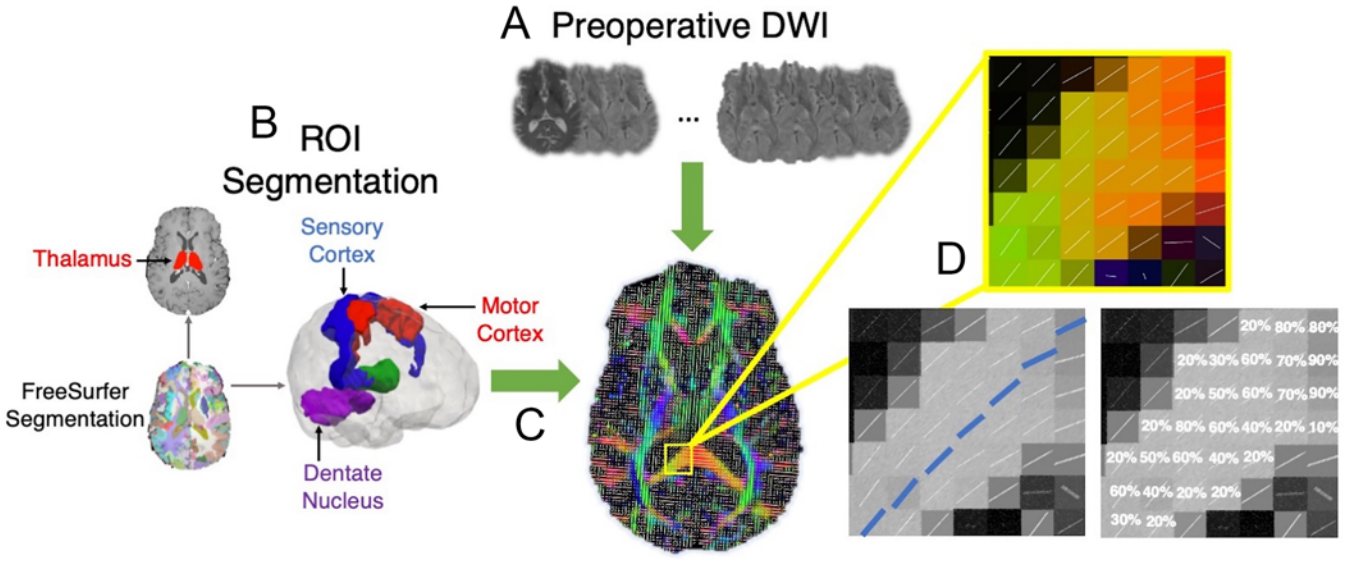


FIG. 1. Region of interest (ROI) definitions and tractography pipeline for use of deterministic and probabilistic tractography. Diffusion images were corrected for motion artifacts and eddy currents (**A**). Motor, sensory, cerebellar white matter, and subcortical masks were created (**B**) and registered to DWI space (**C**). Deterministic and probabilistic fiber tracking were performed to create TDIs and PMs, respectively. Deterministic tractography assumed a single orientation at each voxel, whereas probabilistic tractography assumed a distribution of orientations (**D**).

mize patient comfort, a standardized general anesthetic protocol of induction medications, sevoflurane concentration, hemodynamic parameters (e.g., mean arterial pressure), and respiratory parameters (e.g., end-tidal carbon dioxide level, respiratory rate, oxygen concentration, tidal volume) was instituted for all scans. All patients were scanned on a 3-T Philips Achieva scanner with an 8-channel head coil. For the purposes of segmentation and DBS trajectory planning, patients underwent T2-weighted, proton density–weighted, and gadolinium-enhanced T1-weighted imaging.

Structural scans were acquired using the scanning parameters mentioned in a previous study.[21] DWI was acquired axially in the same anatomical location used for T1-weighted imaging (32 diffusion-encoding directions; b = 850 sec/mm^2; TR 12 msec; TE 83 msec; matrix size 128 × 128; voxel size 2.0 × 2.0 × 2.0 mm^3). The average acquisition time was 15 minutes for DWI, with a total scan time of approximately 50 minutes.

Manual and Semimanual Segmentation of Regions of Interest

For each patient, the left and right thalamus initially underwent automated atlas-based segmentation with CranialSuite.[22] Cortical reconstruction and volumetric segmentation of each patient's individual T1-weighted volume (1-mm isotropic resolution) was performed with the FreeSurfer image analysis suite.[23] Cortical volumetric masks of the hand motor region,[24] primary sensory cortex, and cerebellar white matter of the dentate nucleus were generated. Cerebellar masks of the superior cerebral peduncles were manually segmented using ITK-SNAP software and used as exclusion masks (Fig. 1).[25] One of the authors (C.M.M.) manually supervised all automatic reconstructions provided by CranialSuite and FreeSurfer to correct errors introduced by registration and automatic labeling of cortical and subcortical structures.

Diffusion Data Processing and Tractography

Diffusion data were corrected for motion artifacts and eddy current distortions by using the Artefact correction in diffusion MRI (ACID) toolbox.[26] For both tracking methods, VIM was delineated by using the hand motor area as an initiation mask, the ipsilateral thalamus as a waypoint region, the contralateral dentate nucleus as a termination mask, and the cerebral peduncles as an exclusion mask to exclude false-positive streamlines. Similarly, connections with VC were delineated by using the sensory areas as an initiation mask, the ipsilateral thalamus as a waypoint, the cerebral peduncles as an exclusion mask, and the dorsal columns of the spinal cord set as a termination mask.

The average time needed to obtain estimates for probabilistic tractography using a graphics processing unit (GPU) cluster was approximately 30 minutes. Probabilistic fiber tractography was generated with the Diffusion Toolbox (FDT) of FMRIB Software Library. Distributions of fiber orientations were estimated for each voxel on the basis of the results of the BedpostX tool (FSL version 6.0) of FDT, which computed three crossing fibers per voxel. Streamlines were generated by using local samples of voxel-wise principal diffusion distributions to build a spatial connectivity distribution that described the probability of a path between any two distant points through the diffusion field.[27] The probability maps (PMs) of VIM and VC were extracted as an output of Probtrackx to generate a thalamic map depicting the areas with a high density of probabilities connecting to the motor and sensory areas. To reduce spurious findings, both deterministic and probabilistic track-density maps consisted of voxels with 10%

Brought to you by Thomas Jefferson University | Unauthenticated | Downloaded 10/07/26 03:23 PM UTC

A

	Indirect Target		Planned Target		Implanted Electrode	
	Mean	SD	Mean	SD	Mean	SD
Distance to third ventricle wall (X), mm	10.5	0.0	10.4	0.6	10.7	0.9
Anterior-posterior coordinate* (Y), mm	-6.4	0.4	-7.1	0.9	-7.2	1.1

*AC-PC: anterior commissure-posterior commissure, *relative to midcommissural point*

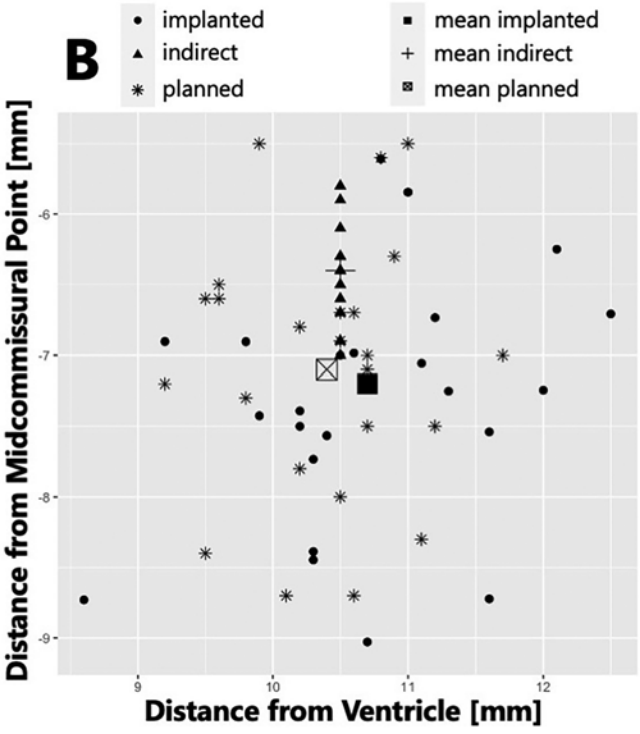


FIG. 2. A: Comparisons of indirect target, final planned target, and implanted electrode positions. **B:** Plot of indirect target (*triangles*), planned target (*asterisks*), and final electrode (*dots*) positions in anterior commissure–posterior commissure coordinates relative to the distance from the lateral ventricle. All points were plotted at the level of the midcommissural plane. The mean coordinates of the indirect target (*plus sign*), planned target (*crossed square*), and final electrode (*black square*) positions are shown.

or less of the highest voxel intensity within the thalamus.[28] This created an artificial separation between the VIM and VC that cannot be observed in anatomical specimens.

Preoperative Trajectory Planning

Trajectory planning was initiated by first selecting the indirect target for VIM, which can be found at one-quarter of the intercommissural distance between the anterior commissure and posterior commissure, 10.5 mm lateral to the lateral wall of the third ventricle, and at the level of the intercommissural plane.[29,30] The target was modified by using probabilistic tractography to optimize a trajectory through the highest probability voxels of the VIM PM that was in proximity to the indirect target, while also completely avoiding the VC PM. The target was extended below the level of the intercommissural plane because all patients underwent segmented electrode implantation to allow for current steering. Therefore, the first segmented contact was implanted at the level of the midcommissural plane (with the deepest contact below the thalamus) in order to leverage current steering within the thalamus. Given the known success of using indirect targeting for image-guided, image-verified DBS as a treatment of ET,[31] efforts were also made to avoid target modifications greater than 2 mm. The entry point was selected just posterior to the coronal suture and modified to maximize cannulation of the VIM PM. Final adjustments were made to avoid blood vessels, to avoid sulci, and to remain at least 4 mm away from the lateral ventricle.[7]

Image-Guided, Image-Verified DBS

Patients underwent robot-assisted, image-guided, image-verified DBS implantation. The planned trajectories were first transferred to the stereotactic robot (Renishaw). Patients were then placed under general endotracheal anesthesia before placement of a Leksell head frame (Elekta). Each patient was supine on the operating room table, and their head was secured to the robot via the Leksell frame. After the registration procedure, two test trajectories were used as verification.

For each trajectory, the robot was used to plan the incision before a 3.2-mm-diameter burr hole was drilled with the guidance of the robotic arm. A 1.6-mm-diameter radiofrequency probe was advanced through the robotic arm along the planned trajectory while dynamic impedances were measured to estimate the probe position relative to gray and white matter. The radiofrequency probe was then exchanged with the DBS electrode under fluoroscopic guidance. The stylet from the electrode was removed before the electrode was secured to the skull with a cranial mini-plate. The final positions of the electrodes were confirmed with intraoperative cone-beam CT. Figure 2 demonstrates the average coordinates based on indirect targeting, the planned coordinates modified after inclusion of tractography data, and the implanted electrode error relative to the planned coordinates.

Patients underwent routine follow-up and programming optimization after DBS implantation. Documentation of postoperative tremor improvement was either qualitative

Brought to you by Thomas Jefferson University | Unauthenticated | Downloaded 10/07/26 03:23 PM UTC

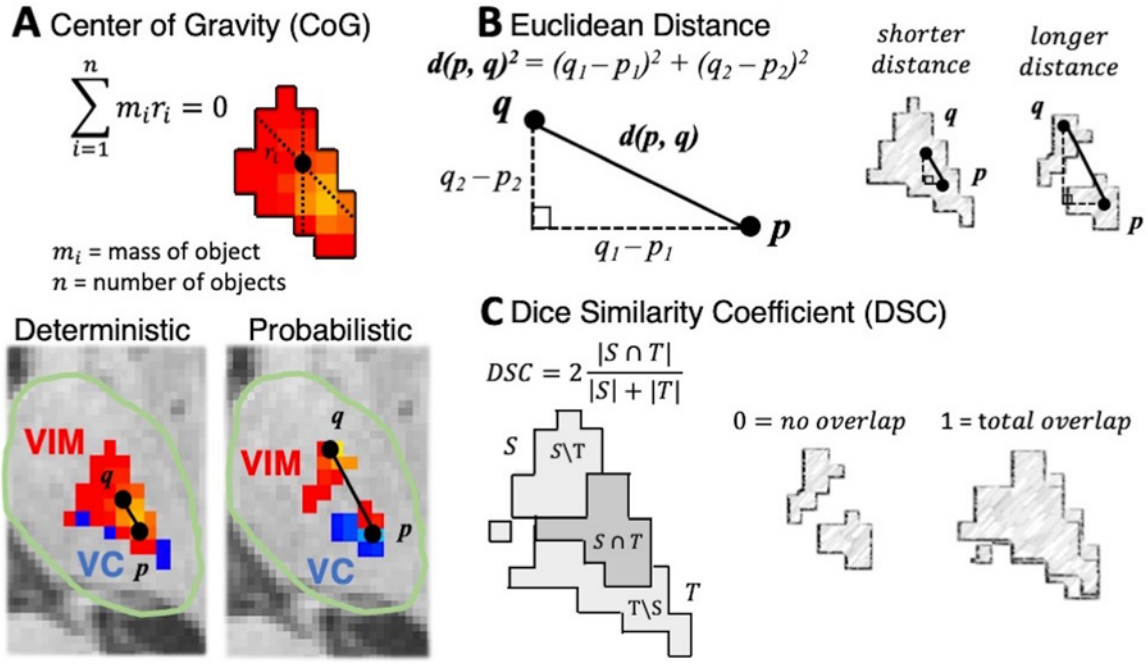


FIG. 3. TDI analysis, including calculation of the location of each CoG, was performed by weighing the average of the coordinates by the intensities within the TDI (equivalent to the concept of center of gravity for an object with a distributed mass, where intensity is substituted for mass in the case of image analysis) (**A**). Quantitative measures, including the Euclidean distance between CoGs (**B**) and the DSC of the tract-density maps (**C**), were determined.

or consisted of postoperative TETRAS scores that quantified the degree of improvement with DBS.

Deterministic Tractography

Preoperative deterministic tractography was performed on all patients for comparison with prospective probabilistic tractography used for presurgical targeting. For deterministic tractography, the MRtrix toolbox (https://github.com/jdtournier/mrtrix3) was used to analyze the diffusion-sensitized data set and to generate fiber orientation distribution estimates with a tensor-free constrained spherical deconvolution model. The same segmented motor and sensory areas used for probabilistic tractography were used as initiation seeds for deterministic tractography with similar methods. We randomly initiated 5000 streamlines from the seed regions covering the motor or sensory cortex, and these were constrained by the aforementioned target, inclusion, and exclusion masks. The result was a set of deterministic streamlines for both the VIM and VC of each patient.

Track-density images (TDIs) of the left and right thalamic streamlines of both motor and sensory fibers were generated using a streamline-counting approach. The number of streamlines passing through a given intersected voxel was counted and mapped as a numerical value. We masked the TDIs to generate a thalamic map depicting thalamic areas with a high density of streamlines connecting the motor and sensory areas.

Comparisons Across and Within Tracking Methods

We compared deterministic and probabilistic methods to quantify separation between VIM and VC. Significant overlap between VIM and VC was observed in the resulting PMs created with deterministic tractography, even prior to thresholding. Therefore, in addition to rendering deterministic PMs for use during presurgical planning, we could not use the same method for direct targeting and thereby draw comparisons between tracking methods. We calculated a weighted sum of the centers of gravity (CoGs) to quantify variance between the two methods, similar to previous methods.[21] CoG is equivalent to the concept of the center of gravity of an object with a distributed mass, but intensity is substituted for mass in the context of imaging analysis (Fig. 3A). CoG is skewed by imaging intensity, rather than by the highest voxel intensity or the anatomical center of the structure, but takes into account density within the region. This is a common method for quantifying tract differences between methods or groups, or longitudinally within individuals.[16,32] To quantify separation between VIM and VC, we calculated the distances (in the x-, y-, and z-directions) between the CoGs of each region (Fig. 3B). Additionally, the Dice similarity coefficient (DSC) between VIM and VC was calculated for each tracking method as a means to quantify the degree of overlap between TDIs and PMs (Fig. 3C). DSC is a widely used measure in medical imaging studies that is calculated to quantify the degree of overlap between two segmented objects, with 1 representing a perfect match between segmentations and 0 indicating no overlap.[33] The independent-samples t-test was applied to compare distances and DSCs between tracking solutions.

Comparison With Indirect Targeting

To provide a reference to indirect targeting, we exam-

Brought to you by Thomas Jefferson University | Unauthenticated | Downloaded 10/07/26 03:23 PM UTC

TABLE 2. Patient TETRAS scores determined while both on and off DBS (n = 9)

Clinical Outcomes	Mean ± SD (range)
Follow-up duration, days	263 ± 212 (42–629)
TETRAS score	
Off DBS	18.2 ± 4.5 (10.0–24.5)
On DBS	5.9 ± 2.2 (3.0–9.5)
Improvement, %	68.0 ± 6.5 (54.8–80.0)

ined the distances between the CoGs determined with the probabilistic and deterministic methods by using indirect atlas-based targets, as described above.[29] For each patient and tracking method, the Euclidean distances and distances along the x- and y-axes between the VIM and VC CoGs and the indirect target were measured along the axial slice.

Results

Patients

Preoperative scanning, planning, and image-guided, image-verified DBS implantation were performed without adverse events, with an average follow-up of 8.6 months. Some patients underwent programming and subsequent follow-up with a movement disorder specialist outside our institution; as such, both preoperative assessment and postoperative assessment after programming optimization were available for only 9 patients, who had a mean TETRAS score improvement of 68%. All patients showed ≥ 54.8% improvement in tremor after DBS, and 1 patient showed 80% improvement in TETRAS score (Table 2). The remaining patients had qualitative tremor improvement and were satisfied with the results of DBS. Although some patients reported transient paresthesias or dizziness associated with stimulation, these symptoms resolved in all patients and there were no persistent stimulation-induced adverse effects.

Detailed programming parameters were available for 14 patients, for whom the average settings consisted of stimulation focused around the two middle electrode contacts, an amplitude of 1.89 mA, frequency of 160 Hz, and pulse width of 56 μsec (Table 1). Current steering was implemented for directional stimulation in 48.1% of patients.

Tractographic Analysis of VIM and VC

Probabilistic methods successfully delineated the pathways of the motor and sensory cortex and the thalamus in 14 patients and across all 60 nuclei. In 1 of 14 patients, deterministic methods failed to delineate any connections from the sensory areas to the thalamus (Fig. 4, patient 10).

Comparison of Tracking Solutions

In general, the deterministic method reconstructed narrow and sparse bundles of streamlines that originated from smaller and more variable areas of the motor and sensory cortex. Overall, prior to thresholding, the proba-

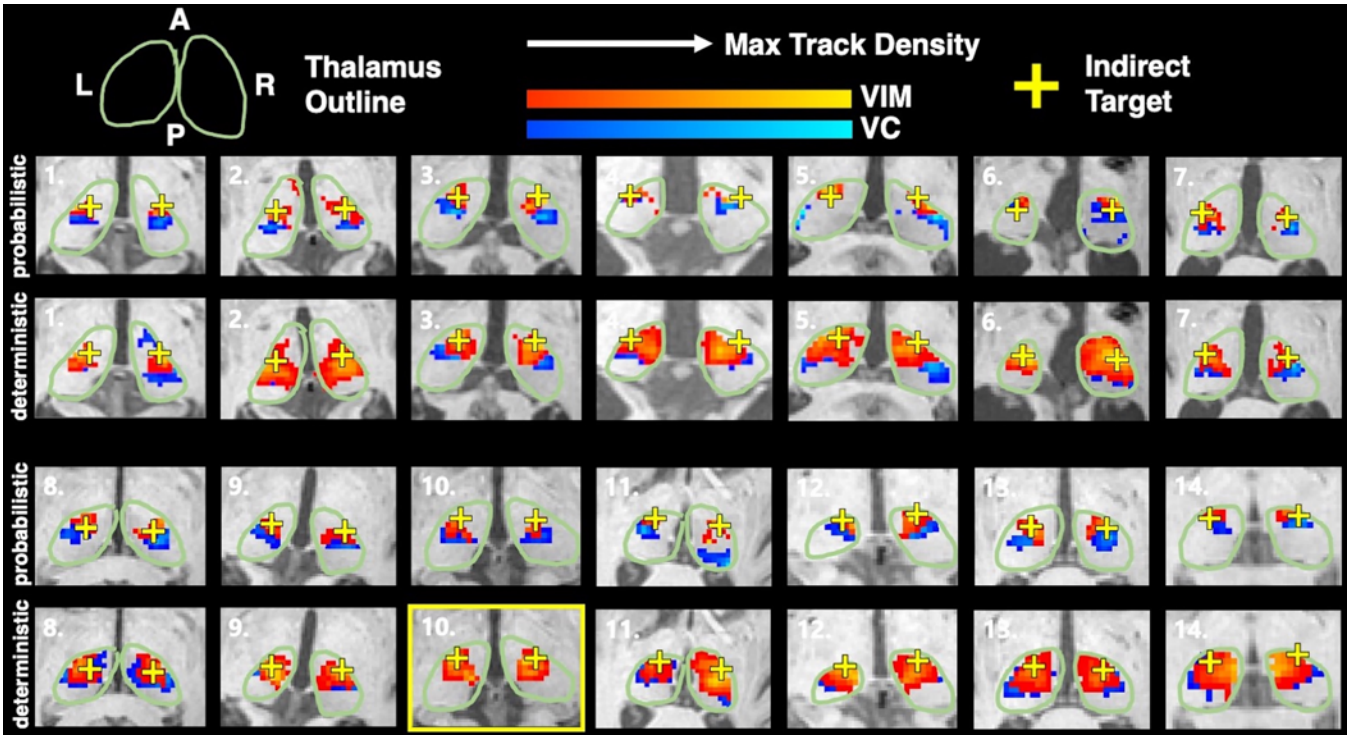


FIG. 4. Axial slices of TDIs of VIM and VC for all patients, as determined with probabilistic and deterministic tractography. Both tractography methods consistently found the CoG to be more lateral and posterior than the indirect target. The deterministic method failed to generate VC fibers in patient 10 (*highlighted*).

Brought to you by Thomas Jefferson University | Unauthenticated | Downloaded 10/07/26 03:23 PM UTC

bilistic method reconstructed a more continuous set of streamlines that projected from the thalamus and a larger area of motor and sensory regions; after thresholding, the probabilistic method identified fibers with less sensitivity but greater specificity than the deterministic method. All reconstructions of both methods appeared to connect motor fibers with the ventrolateral aspect of the thalamus, and sensory fibers with the ventral posterior lateral nucleus. Euclidean distances differed considerably between tracking methods and within patients for the same nucleus; CoG coordinate differences were as large as 4.9 mm and more than half differed by > 2.5 mm (Table 3). The probabilistic method consistently identified VIM fibers to be more anterior, lateral, and superior than fibers identified with the deterministic method, and VC fibers identified with the probabilistic method were consistently more posterior, lateral, and superior than fibers identified with the deterministic method (Fig. 4).

Delineation of VIM and VC With Different Tracking Methods

When the Euclidean distances between VIM and VC were compared, the separation between CoGs determined with the probabilistic method was nearly twice as large as that determined with the deterministic method. On average, the probabilistic method detected VIM to be 2 mm more anterior than VC, whereas the deterministic method detected distances of separation that were an average of 1 mm more anterior (Table 3).

Comparison With Indirect Targeting

Both probabilistic and deterministic methods found that VIM CoG was more lateral, posterior, and superior relative to the atlas-based reference. Patient-specific anatomy and the locations of the probabilistic tracts caused the planned targets to be, on average, more posterior (0.64 ± 1.01 mm) and more lateral (0.30 ± 0.96 mm). There was also increased variability in the target coordinates when the probabilistic method was used: the x-axis coordinate ranged from 1.24 medial to 2.49 mm lateral of the indirect target, and the y-axis coordinate ranged from 1.49 mm anterior to 2.71 mm posterior of the indirect target. The mean ± SD (range) radial distance between the planned target and the indirect target on the intercommissural plane was 1.33 ± 0.79 (0.06–2.76) mm.

The probabilistic CoG of VIM was consistently further from the indirect target than the deterministic CoG by approximately 1–2 mm (Table 3).

Delineation of the Target and No-Go Region

Although fewer fibers were detected after thresholding, the probabilistic method demonstrated significantly clearer delineation of VIM from VC, as determined according to the DSCs ($p < 0.001$). CoG distances between the VIM and VC ranged from 1.4 to 5.4 mm according to the deterministic method, versus 2.8 to 7.3 mm with the probabilistic method (Table 3). Moreover, the DSC of the deterministic method was significantly greater ($p < 0.001$), meaning that the deterministic method found more overlap between motor and sensory fibers than the probabilistic method.

TABLE 3. Mean distances of the CoGs along the axial slice and Euclidean distances

Tracking Method	x-Axis Distance (mm)*	y-Axis Distance (mm)†	Euclidean Distance (mm)
CoG btwn tracking methods			
VIM (n = 14)	−0.43	0.54	2.44
VC (n = 13)	−0.41	−0.60	2.28
Delineation of VIM & VC (n = 13)			
Deterministic CoG			
VIM to VC	0.59	0.95	2.78
Probabilistic CoG			
VIM to VC	0.64	2.16	5.05
VIM CoG w/ indirect target‡			
Deterministic (n = 14)	−0.79	−0.81	8.18
Probabilistic (n = 14)	−1.85	−1.68	9.48

* Values are shown from medial (positive) to lateral (negative).
† Values are shown from anterior (positive) to posterior (negative).
‡ The large Euclidean distances between the VIM CoG and the indirect target were largely due to the former being located more superior. A trajectory that extended through the VIM CoG to the level of the indirect target was on average 1.13 mm (probabilistic) or 2.5 mm (deterministic) posterior and lateral to the indirect target.

Discussion

To the best of our knowledge, this is the first report of the use of prospective direct targeting of VIM with probabilistic tractography in ET patients undergoing DBS. This approach allowed us to achieve on average 68.0% tremor reduction in patients after image-guided, image-verified DBS, with no adverse events or persistent stimulation-induced adverse effects. During the initial programming session, the amplitude was typically increased to 3–5 mA; however, if greater values did not provide additional therapeutic benefit, the minimal amplitude necessary to achieve maximal therapeutic benefit was set in order to minimize battery consumption. It is notable that these results were achieved with average stimulation amplitudes less than 2 mA and pulse widths less than 60 μsec, and the majority of the programs were not directional in nature. These parameters suggest that larger volumes of tissue activation were not required to overcome suboptimal electrode position. In addition to presenting the first prospective targeting study, we present the first systematic comparison of probabilistic and deterministic tractography for delineation of VIM and VC in patients with ET undergoing DBS and highlight the clinical significance of probabilistic fiber tractography for preoperative VIM targeting.

Probabilistic Versus Deterministic Tractography

The VIM is approximately 4 × 4 × 6 mm in size, bordered posteriorly by the VC, and located in the inferior part of the ventral posterolateral nucleus.[34–36] The VIM is centrally placed in the cerebello-thalamo-cortical network, which is likely modulated by DBS through pathologic activity for successful tremor control.[37] We found

Brought to you by Thomas Jefferson University | Unauthenticated | Downloaded 10/07/26 03:23 PM UTC

that probabilistic fiber tracking was both more sensitive and more specific than deterministic tractography for separating areas of VIM and VC in all patients. This can be easily appreciated when examining the resulting maps shown in Fig. 4. Although the probabilistic method delineated boundaries between VIM and VC, the deterministic method often demonstrated overlap; for patient 10, the deterministic method failed to reconstruct fibers altogether. Qualitatively, probabilistic methods detected the CoG of VIM to be more anterior and lateral, and VC to be more posterior and medial, than the deterministic methods by an average of 1–2 mm. Quantitatively, probabilistic tractography was able to estimate the probability that a white matter tract would pass through a given voxel in the brain.[27] Therefore, more widespread detection of fibers within the target region was observed with this technique, demonstrating that probabilistic tractography is more sensitive than deterministic tractography for detecting both dominant and nondominant fiber pathways.

Distance From Indirect Targets

Traditionally, identification of VIM relies on atlas-defined coordinates in relation to the anterior and posterior commissures as landmarks, along with other identifiable structures such as the lateral border between the thalamus and internal capsule border.[5] However, this method fails to account for individual variability; therefore, we postulate that atlas-based targeting may be a more conservative trajectory-planning method that results in a VIM location that is more medial to avoid the internal capsule and more anterior to avoid the VC. This hypothesis helps to explain why indirect targeting during asleep DBS for patients with ET has been shown to be effective, too.[30] We found that both probabilistic and deterministic targeting provided locations that were more lateral and posterior than conventional indirect coordinates, with probabilistic targets located even more lateral and posterior than deterministic targets (Table 3). This difference directly influenced surgical planning, which consisted of targets that were more lateral and posterior than the indirect target. Therefore, it is possible that the ideal target for VIM may be more lateral and posterior than the location provided by traditional targeting methods; this is supported by the clinical results of our patients, all of whom received good therapeutic effect (Table 2). Furthermore, recent studies of VIM targeting based on direct visualization with proton density–weighted MRI reported more lateral targeting,[38] equivalent functional outcomes, and fewer stimulation- and speech-related adverse effects than historical cohorts.[30]

The large Euclidean distances between the tract-based CoGs and indirect targets were largely due to the more superior locations of the CoGs. At the same time, one must remember that the indirect target is intended to be the termination point of the DBS electrode, such that electrodes implanted at the indirect target would pass the tract-based CoGs anteriorly and medially by an average of 1.13 mm (with the probabilistic method) or 2.5 mm (deterministic method).

Clinical Utility of Probabilistic Tractography

Probabilistic tracking resulted in more constrained and reliable tracking of cerebellar-thalamic fibers in patients with ET than deterministic tracking.[2] The results of this study hold large implications for the clinical adoption of probabilistic tractography–based targeting, because reliable, consistent delineation of VIM and VC may avoid complications that result from accidental stimulation of sensory fibers.[10] Moreover, it has been wrongly assumed that deterministic tractography algorithms produce fewer false-positive results and are more suitable for surgical planning in some patients, with probabilistic tractography providing no additional benefit for the resolution of crossing fibers.[39] Our results suggest that probabilistic tractography is significantly better for the separation of VIM and VC, both quantitative and qualitatively, because the CoG distances between VIM and VC were consistently greater according to probabilistic tractography (Table 3); in addition, probabilistic tractography provided significantly less overlap between TDIs as determined according to the DSC values (Fig. 5B). Such large discrepancies between these two diffusion-based methods can be largely attributed to the inherent spatial resolution of DWI, which relies on echo-planar imaging that is intrinsically limited to 2–3 mm of isotropic resolution. This limited resolution is generally inadequate for identifying anisotropic information, particularly in a region that contains many overlapping relay points and inputs, such as the thalamus.[4] Therefore, a tracking method that can resolve the issue of crossing and diverging fibers is essential for mapping thalamic subdivisions.

Previous studies have compared the performance of probabilistic over deterministic methods for presurgical targeting of the subthalamic nucleus[16] and globus pallidus internus.[21] However, to date, no study has provided a systematic comparison of probabilistic with deterministic tractography for the purpose of distinguishing VIM and VC in patients with ET.[39] Additionally, although previous studies have determined retrospective correlations between clinical outcomes and connectivity-based segmentation of the VIM and thalamus,[40] none used tractography for prospective target selection. Our study compared prospective tractography methods for VIM and VC delineation that used consistent imaging parameters and acquisition methods, clinically feasible scanning parameters, and postprocessing methods available at the majority of centers.

Limitations and Future Work

Although our study demonstrated both the feasibility and precision of probabilistic tractography for VIM targeting, this technique is not without limitations. Probabilistic tractography can be computationally cumbersome and time consuming. Estimation of the number of crossing fibers per voxel can take up to 15 hours without batch processing.[41] Such processing could be incorporated into the workflows of surgeons who routinely plan trajectories prior to the day of surgery, but this would not be easily accommodated by those who routinely perform stereotactic planning immediately prior to the surgical procedure. Technological advances in processing capabilities, such as GPU processing, may help shorten processing duration. As more centers recognize the advantages of advanced

Brought to you by Thomas Jefferson University | Unauthenticated | Downloaded 10/07/26 03:23 PM UTC

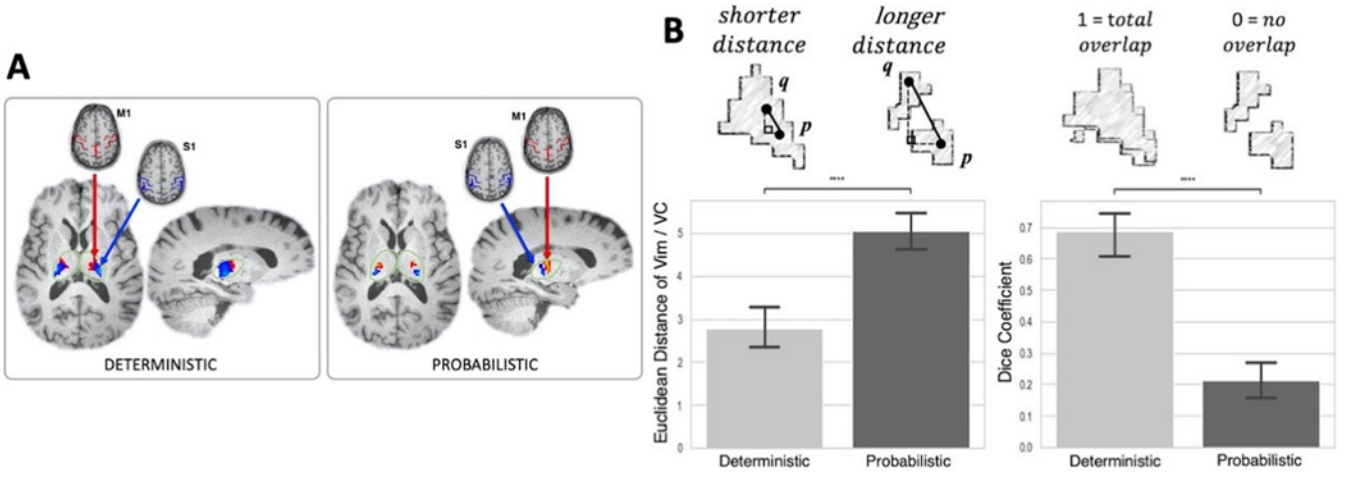


FIG. 5. Axial and sagittal views of deterministic and probabilistic TDI maps used for prospective VIM targeting, with the corresponding cortical masks used in 1 representative patient. The primary sensory area (S1 [*blue*]) and hand motor area (M1 [*red*]) are shown (**A**), as well as the Euclidean distances and DSC calculations between VIM and VC. The probabilistic method had significantly greater Euclidean distances ($p < 0.001$) and significantly less overlap ($p < 0.001$), as determined with the independent-samples t-test (**B**). *Bars* indicate mean values, and *error bars* indicate standard deviation.

targeting techniques, appropriate software and computing power may become more available for clinical use.

Future studies are needed that incorporate modeling of stimulation fields and long-term outcomes of patients who underwent tractography-based planning in order to better understand the clinical significance of probabilistic tractography. In future work, we intend to analyze the relationships between PMs and electrode placement in order to quantify the effect of probabilistic tractography on clinical outcomes beyond presurgical planning. Lastly, prospective multiinstitutional collaboration would greatly speed the acquisition and translation of tractography into the clinical setting.[4]

Conclusions

Advanced preoperative targeting of the motor thalamus has the potential to improve accuracy for known functional and anatomical targets, advance our understanding of the pathophysiology of tremor, and move the field toward the next stage in the evolution of DBS targeting. In this study, we demonstrated the safety and efficacy of our early experience using prospective probabilistic tractography–based targeting of VIM for image-guided, image-verified DBS in ET patients under anesthesia. In addition, we have shown how probabilistic tractography allowed for greater separation of VIM and VC fibers within a clinically feasible time frame.

References

1. Meng FG, Zhang JG, Kao CC, Klein JC, Hilker R. The tremor network targeted by successful VIM deep brain stimulation in humans. *Neurology*. 2012;79(9):953.
2. Schlaier JR, Beer AL, Faltermeier R, Fellner C, Steib K, et al. Probabilistic vs. deterministic fiber tracking and the influence of different seed regions to delineate cerebellar-thalamic fibers in deep brain stimulation. *Eur J Neurosci*. 2017;45(12):1623-1633.
3. Al-Fatly B, Ewert S, Kübler D, Kroneberg D, Horn A, Kühn AA. Connectivity profile of thalamic deep brain stimulation to effectively treat essential tremor. *Brain*. 2019;142(10):3086-3098.
4. Gravbrot N, Saranathan M, Pouratian N, Kasoff WS. Advanced imaging and direct targeting of the motor thalamus and dentato-rubro-thalamic tract for tremor: a systematic review. *Stereotact Funct Neurosurg*. 2020;98(4):220-240.
5. Akram H, Dayal V, Mahlknecht P, Georgiev D, Hyam J, et al. Connectivity derived thalamic segmentation in deep brain stimulation for tremor. *Neuroimage Clin*. 2018;18(18):130-142.
6. Deistung A, Schäfer A, Schweser F, Biedermann U, Turner R, Reichenbach JR. Toward in vivo histology: a comparison of quantitative susceptibility mapping (QSM) with magnitude-, phase-, and R2*-imaging at ultra-high magnetic field strength. *Neuroimage*. 2013;65:299-314.
7. Burchiel KJ, McCartney S, Lee A, Raslan AM. Accuracy of deep brain stimulation electrode placement using intraoperative computed tomography without microelectrode recording. *J Neurosurg*. 2013;119(2):301-306.
8. Chen T, Mirzadeh Z, Chapple KM, Lambert M, Evidente VGH, et al. Intraoperative test stimulation versus stereotactic accuracy as a surgical end point: a comparison of essential tremor outcomes after ventral intermediate nucleus deep brain stimulation. *J Neurosurg*. 2018;129(2):290-298.
9. Behrens TEJ, Johansen-Berg H, Woolrich MW, Smith SM, Wheeler-Kingshott CA, et al. Non-invasive mapping of connections between human thalamus and cortex using diffusion imaging. *Nat Neurosci*. 2003;6(7):750-757.
10. Jakab A, Werner B, Piccirelli M, Kovács K, Martin E, et al. Feasibility of diffusion tractography for the reconstruction of intra-thalamic and cerebello-thalamic targets for functional neurosurgery: a multi-vendor pilot study in four subjects. *Front Neuroanat*. 2016;10:76.
11. Jakab A, Blanc R, Berényi EL, Székely G. Generation of individualized thalamus target maps by using statistical shape models and thalamocortical tractography. *AJNR Am J Neuroradiol*. 2012;33(11):2110-2116.
12. Johansen-Berg H, Behrens TEJ, Sillery E, Ciccarelli O, Thompson AJ, et al. Functional-anatomical validation and individual variation of diffusion tractography-based segmentation of the human thalamus. *Cereb Cortex*. 2005;15(1):31-39.
13. Pouratian N, Zheng Z, Bari AA, Behnke E, Elias WJ, De-

Brought to you by Thomas Jefferson University | Unauthenticated | Downloaded 10/07/26 03:23 PM UTC

salles AAF. Multi-institutional evaluation of deep brain stimulation targeting using probabilistic connectivity-based thalamic segmentation. *J Neurosurg*. 2011;115(5):995-1004.
14. Sammartino F, Krishna V, King NKK, Lozano AM, Schwartz ML, et al. Tractography-based ventral intermediate nucleus targeting: novel methodology and intraoperative validation. *Mov Disord*. 2016;31(8):1217-1225.
15. Lozano AM. Vim thalamic stimulation for tremor. *Arch Med Res*. 2000;31(3):266-269.
16. Petersen MV, Lund TE, Sunde N, Frandsen J, Rosendal F, et al. Probabilistic versus deterministic tractography for delineation of the cortico-subthalamic hyperdirect pathway in patients with Parkinson disease selected for deep brain stimulation. *J Neurosurg*. 2017;126(5):1657-1668.
17. Behrens TEJ, Woolrich MW, Jenkinson M, et al. Characterization and propagation of uncertainty in diffusion-weighted MR imaging. *Magn Reson Med*. 2003;50(5):1077-1088.
18. Jeurissen B, Leemans A, Tournier JD, Jones DK, Sijbers J. Investigating the prevalence of complex fiber configurations in white matter tissue with diffusion magnetic resonance imaging. *Hum Brain Mapp*. 2013;34(11):2747-2766.
19. Descoteaux M, Deriche R, Knösche TR, Anwander A. Deterministic and probabilistic tractography based on complex fibre orientation distributions. *IEEE Trans Med Imaging*. 2009;28(2):269-286.
20. Ondo WG, Pascual B. Tremor Research Group Essential Tremor Rating Scale (TETRAS): Assessing impact of different item instructions and procedures. *Tremor Other Hyperkinet Mov (N Y)*. 2020;10(1):36.
21. Muller J, Alizadeh M, Mohamed FB, Riley J, Pearce JJ, et al. Clinically applicable delineation of the pallidal sensorimotor region in patients with advanced Parkinson's disease: study of probabilistic and deterministic tractography. *J Neurosurg*. 2019;131(5):1520-1531.
22. D'Haese PF, Pallavaram S, Li R, Remple MS, Kao C, et al. CranialVault and its CRAVE tools: a clinical computer assistance system for deep brain stimulation (DBS) therapy. *Med Image Anal*. 2012;16(3):744-753.
23. Dale AM, Fischl B, Sereno MI. Cortical surface-based analysis: I. Segmentation and surface reconstruction. *NeuroImage*. 1999;9(2):179-194.
24. Caulo M, Briganti C, Mattei PA, Perfetti B, Ferretti A, et al. New morphologic variants of the hand motor cortex as seen with MR imaging in a large study population. *AJNR Am J Neuroradiol*. 2007;28(8):1480-1485.
25. Yushkevich PA, Piven J, Hazlett HC, Smith RG, Ho S, et al. User-guided 3D active contour segmentation of anatomical structures: significantly improved efficiency and reliability. *Neuroimage*. 2006;31(3):1116-1128.
26. Mohammadi S, Möller HE, Kugel H, Müller DK, Deppe M. Correcting eddy current and motion effects by affine whole-brain registrations: evaluation of three-dimensional distortions and comparison with slicewise correction. *Magn Reson Med*. 2010;64(4):1047-1056.
27. Behrens TEJ, Woolrich MW, Jenkinson M, Johansen-Berg H, Nunes RG, et al. Characterization and propagation of uncertainty in diffusion-weighted MR imaging. *Magn Reson Med*. 2003;50(5):1077-1088.
28. Kincses ZT, Szabó N, Valálik I, Kopniczky Z, Dézsi L, et al. Target identification for stereotactic thalamotomy using diffusion tractography. *PLoS One*. 2012;7(1):e29969.
29. Osenbach R, Richard K, Burchiel K. Thalamotomy: indications, techniques, and results. In: Germano IM, ed. *Neurosurgical Treatment of Movement Disorders*. AANS; 1998.
30. Ponce FA, Lambert M. 207 Direct targeting of the ventral intermediate nucleus using high-field proton density MR imaging: functional outcomes and comparison to "indirect" targeting. *Neurosurgery*. 2019;66(Supplement 1):65.
31. Chen T, Mirzadeh Z, Chapple K, Lambert M, Dhall R, Ponce FA. "Asleep" deep brain stimulation for essential tremor. *J Neurosurg*. 2016;124(6):1842-1849.
32. Waugh JL, Kuster JK, Makhlouf ML, et al. A registration method for improving quantitative assessment in probabilistic diffusion tractography. *NeuroImage*. 2019:288-306.
33. Zou KH, Warfield SK, Bharatha A, Tempany CM, Kaus MR, et al. Statistical validation of image segmentation quality based on a spatial overlap index. *Acad Radiol*. 2004;11(2):178-189.
34. Abosch A, Yacoub E, Ugurbil K, Harel N. An assessment of current brain targets for deep brain stimulation surgery with susceptibility-weighted imaging at 7 tesla. *Neurosurgery*. 2010;67(6):1745-1756.
35. Hirai T, Jones EG. A new parcellation of the human thalamus on the basis of histochemical staining. *Brain Res Brain Res Rev*. 1989;14(1):1-34.
36. Jones EG. *The Thalamus*. Springer; 2012.
37. Dembek TA, Petry-Schmelzer JN, Reker P, Wirths J, Hamacher S, et al. PSA and VIM DBS efficiency in essential tremor depends on distance to the dentatorubrothalamic tract. *Neuroimage Clin*. 2020;26(March):102235.
38. Morrison MA, Lee AT, Martin AJ, Dietiker C, Brown EG, Wang DD. DBS targeting for essential tremor using intersectional dentato-rubro-thalamic tractography and direct proton density visualization of the VIM: technical note on 2 cases. *J Neurosurg*. 2021;135(3):806-814.
39. Krishna V, Sammartino F, Agrawal P, Changizi BK, Bourekas E, et al. Prospective tractography-based targeting for improved safety of focused ultrasound thalamotomy. *Neurosurgery*. 2019;84(1):160-168.
40. Akram H, Sotiropoulos SN, Jbabdi S, Georgiev D, Mahlknecht P, et al. Subthalamic deep brain stimulation sweet spots and hyperdirect cortical connectivity in Parkinson's disease. *Neuroimage*. 2017;158:332-345.
41. Behrens TEJ, Berg HJ, Jbabdi S, Rushworth MFS, Woolrich MW. Probabilistic diffusion tractography with multiple fibre orientations: What can we gain? *Neuroimage*. 2007;34(1):144-155.

Disclosures

Dr. Liang is an investigator for the Abbott PROGRESS trial.

Author Contributions

Conception and design: Muller, Alizadeh, Matias, Wu. Acquisition of data: all authors. Analysis and interpretation of data: Muller, Alizadeh, Matias, Mohamed, Wu. Drafting the article: Muller, Alizadeh, Matias, Wu. Critically revising the article: Muller, Alizadeh, Matias, Thalheimer, Mohamed, Wu. Reviewed submitted version of manuscript: all authors. Approved the final version of the manuscript on behalf of all authors: Muller. Statistical analysis: Muller, Alizadeh, Wu. Administrative/technical/material support: Thalheimer, Romo, Martello, Liang, Mohamed, Wu. Study supervision: Thalheimer, Romo.

Correspondence

Jennifer Muller: Jefferson Integrated Magnetic Resonance Imaging Center, Thomas Jefferson University Hospital, Philadelphia, PA. jxm491@jefferson.edu.

Brought to you by Thomas Jefferson University | Unauthenticated | Downloaded 10/07/26 03:23 PM UTC